

First and second order magnetic and structural transitions in $\text{BaFe}_{2(1-x)}\text{Co}_{2x}\text{As}_2$

C. R. Rotundu^{1,*} and R. J. Birgeneau^{2,3}

¹*Materials Sciences Division, Lawrence Berkeley National Laboratory, Berkeley, CA 94720, USA*

²*Department of Physics, University of California, Berkeley, CA 94720, USA*

³*Department of Materials Science and Engineering, University of California, Berkeley, CA 94720, USA*

(Dated: May 31, 2022)

We present here high resolution magnetization measurements on high-quality $\text{BaFe}_{2(1-x)}\text{Co}_{2x}\text{As}_2$, $0 \leq x \leq 0.046$ as-grown single crystals. The results confirm the existence of a magnetic tricritical point in the (x, T) plane at $x_{tr}^m \approx 0.022$ and reveal the emergence of the heat capacity anomaly associated with the onset of the structural transition at $x^s \approx 0.0064$. We show that the samples with doping near x_{tr}^m do not show superconductivity, but rather superconductivity emerges at a slightly higher cobalt doping, $x \approx 0.0315$.

PACS numbers: 74.25.Dw, 74.25.Bt, 74.70.Db, 74.62.Bf, 64.60.Kw

The 122 series (AFe_2As_2 , $\text{A} = \text{Ba, Sr, Ca, Eu}$) is one of the most studied among the newly discovered iron arsenide high temperature superconductors. One intriguing fact is that in this series superconductivity can be induced by doping in any of the three atomic sites; the cobalt doped system $\text{BaFe}_{2-2x}\text{Co}_{2x}\text{As}_2$ ^{1,2} is, for instance, one of the most studied systems. The antiferromagnetic (spin-density wave) and structural (tetragonal to orthorhombic) transitions that are near-coincident in the parent compounds³ are concomitantly and gradually suppressed upon doping. A large number of papers have been written on the thermodynamic nature of the transitions in 122s arguing for either 1st order or 2nd order phase changes. If we solely consider the BaFe_2As_2 system, reports range from both 2nd order structural and magnetic phase transitions³, to both transitions 2nd order but with the possibility of magnetic 1st order transition within 0.5 K of T_N ⁴, to 1st of a order magnetic transition⁵, to indiscernibility between the two scenarios for the magnetic phase transition (did not see either the abrupt change at T_N of the magnetic order parameter that is expected for a first-order transition, or the divergence of the correlation length at T_N that would suggest a second-order transition)⁶.

More recent combined high resolution X-ray diffraction and heat capacity measurements on exceptionally high quality BaFe_2As_2 crystals revealed a 1st order magnetic transition preceded by a structural transition that starts as a 2nd order transition at a slightly higher temperature but with a first order jump in the orthorhombic distortion coincident with the first order magnetic transition⁷. Since data on some doped Ba122 samples show clear 2nd order magnetic and structural transitions⁸⁻¹⁰, it has been theoretically suggested that the magneto-structural transition in the parent is close to a tricritical point¹¹ that is tunable through doping. The only exception appears to be the case of the hole-doped $\text{Ba}_{1-x}\text{K}_x\text{Fe}_2\text{As}_2$ for which both the magnetic and structural transitions seem to be 1st order over the entire phase diagram¹². Further, ARPES measurements on cobalt doped Ba122 evidenced a Lifshitz transition at the onset of superconductivity¹³,

while high-resolution x-ray diffraction and x-ray resonant magnetic scattering (XRMS) pointed to a magnetic tricritical point at $x \approx 0.022$, but with a structural transition whose onset is 2nd order across the whole cobalt doping range¹⁴.

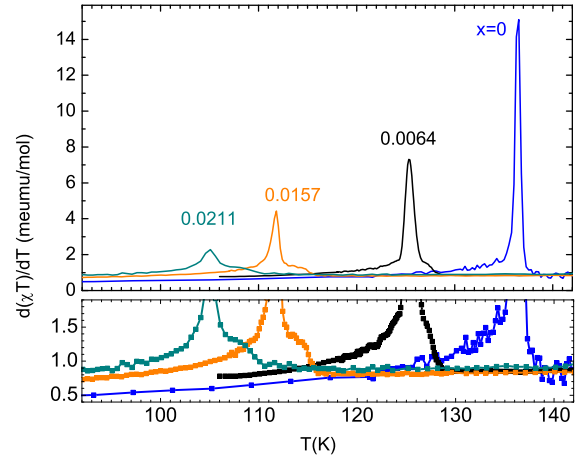


FIG. 1: $d(\chi T)/dT$ versus T of the $\text{BaFe}_{2(1-x)}\text{Co}_{2x}\text{As}_2$, $0 \leq x \leq 0.0211$ crystals. The higher temperature shoulder corresponds to the structural transition and the lower peak to the magnetic transition. The lower panel shows the same data near the “base” of the peaks on an expanded scale.

Magnetic and structural order parameters are normally obtained through scattering measurements. At the same time, measurements of thermodynamic quantities such as the heat capacity give direct information about the fluctuations associated with the order parameters and they can often be performed with quite high precision¹⁵. For instance, fittings of high resolution heat capacity data in the critical region of a second order transition¹⁶ can give information about the values of the critical expo-

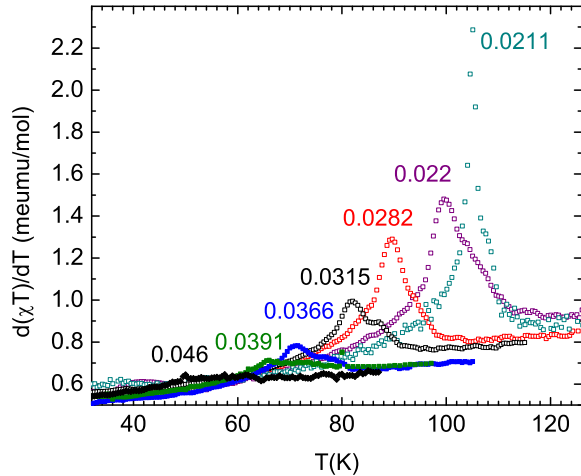


FIG. 2: $d(\chi T)/dT$ versus T of the as-grown crystals $\text{BaFe}_{2(1-x)}\text{Co}_{2x}\text{As}_2$, $0.0211 \leq x \leq 0.046$.

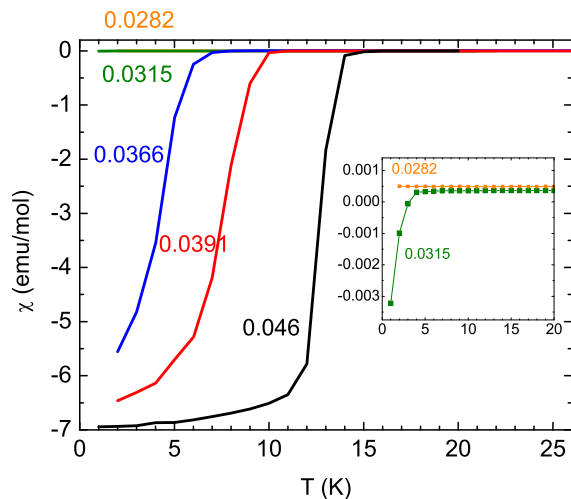


FIG. 3: Magnetic susceptibility χ versus T of $\text{BaFe}_{2(1-x)}\text{Co}_{2x}\text{As}_2$ for cobalt doping $x=0.0282$, 0.0315 , 0.0366 , 0.0391 , and 0.046 measured in 20 Oe. The inset shows in magnified scale only the data of samples $x=0.0282$ and 0.0315 .

nents and therefore on the dimensionality and symmetry of the systems under investigation. In the particular case of the 122s, because of the proximity of the magnetic and structural transitions, fits of the data near the transitions cannot be done reliably. Heat capacity measurements have been successfully used in the study of systems exhibiting doping driven *first-to-second* order change of the transition^{17–19}. In these cases, high resolu-

tion heat capacity measurements, for instance, through a precise accounting of the latent heat²⁰, can determine the order of the transition extremely close to a tricritical point^{21,22}. However, these kinds of high resolution heat capacity measurements require a special setup and are very difficult to perform.

In this article we make use, rather, of the general theoretical argument of M. E. Fisher²³ that shows that “the variation of the magnetic specific heat of a *simple* antiferromagnet, in particular the singular behavior in the region of the transition, should be closely similar to the behavior of the function $\partial(\chi T)/\partial T$, here χ is the zero-field susceptibility.” The theoretical result had been successfully tested initially on MnO and MnF_2 ²³. Although this theoretical result was initially meant for antiferromagnetic transitions, it seems that $\partial(\chi T)/\partial T$ mimics C for both the magnetic and structural transitions of Co-doped Ba122 itself², other 122s and 1111s as well. While establishing a precise equivalence between $C(T)$ and $\partial(\chi T)/\partial T(T)$ is beyond the present study, we will exploit here the direct proportionality between the two physical measures at the transitions, i.e.

$$C(T=T_t) \propto \partial(\chi T)/\partial T(T=T_t), \text{ where } T_t = T_N, T_s.$$

The measurements were made on as-grown single crystals of $\text{BaFe}_{2(1-x)}\text{Co}_{2x}\text{As}_2$ that were grown by the self-flux method²⁴. Inductively coupled plasma (ICP) and electron microprobe wavelength-dispersive X-ray spectroscopic (WDS) analysis were used to determine the actual stoichiometry of the samples, particular attention being given to the cobalt content. The samples (as determined by WDS) under study were: $x=0$, 0.0038 ± 0.0006 , 0.0064 ± 0.0005 , 0.0157 ± 0.0007 , 0.0211 ± 0.0005 , 0.0220 ± 0.0005 , 0.0282 ± 0.0010 , 0.0315 ± 0.0011 , 0.0366 ± 0.0015 , 0.0391 ± 0.0011 and 0.046 ± 0.0015 . The \pm represents the standard deviation from the average x value of readings on ten randomly chosen points on each sample. The magnetic susceptibility measurements on the samples were made using a Quantum Design Magnetic Property Measurement System (MPMS) in a magnetic field of 5 T parallel with the $(a b)$ crystallographic plane, unless otherwise noted. The machine was “finely tuned”²⁵ before the measurements to exploit the limits of its sensitivity, and also special care was taken to avoid oxygen contamination^{25,26}.

In brief, we describe high resolution magnetic susceptibility measurements on $\text{BaFe}_{2(1-x)}\text{Co}_{2x}\text{As}_2$, $0 \leq x \leq 0.04$ that confirm the prediction of a magnetic tricritical point at the doping $x \approx 0.022$ and reveal in addition the emergence of the heat capacity anomaly associated with the onset of the second order structural transition at a lower doping, $x \approx 0.0064$. Our data show further that the superconductivity emerges at a higher cobalt doping than the doping that corresponds to the magnetic tricritical point: at $x \approx 0.0315$.

Figures 1 and 2 show $d(\chi T)/dT$ versus T of the as-grown crystals $\text{BaFe}_{2(1-x)}\text{Co}_{2x}\text{As}_2$ for $0 \leq x \leq 0.0211$ and $0.0211 \leq x \leq 0.046$, respectively. For the undoped sample ($x=0$) the corresponding $d(\chi T)/dT$ signature for both

the antiferromagnetic (AFM) and structural transitions in this sample cannot be further apart than 0.25 K. This is consistent with previous results from our group. Given the T_N and T_s dependence on the annealing (therefore synthesis) conditions⁷, it is not surprising that a $(T_s - T_N)$ as large as 0.75 K has been reported¹⁴. Samples with $x=0$ and $x=0.0038$ (data not shown) show a single sharp peak which can be unambiguously identified with the combined magnetic and structural first order transition observed by Rotundu *et al.*⁷ and Kim *et al.*¹⁴. However, the anticipated heat capacity anomaly associated with the initial second order tetragonal-orthorhombic structural transition is not resolvable from the tail of the first order transition. However, as is evident in Fig. 1, for $x=0.0064$ cobalt doping, the heat capacity signature associated with the second order structural peak first emerges as a subtle but clear shoulder on the high temperature side of the first order jump (lower panel of Fig. 1).

Figure 3 shows magnetic susceptibility χ versus T of $\text{BaFe}_2(1-x)\text{Co}_{2x}\text{As}_2$ for cobalt doping $x=0.0282$, 0.0315, 0.0366, and 0.0391 measured in 20 Oe. Samples $x=0.022$ and 0.0282 show a positive low temperature magnetization and therefore no signs of superconductivity. For sample $x=0.0315$, although χ shows a clear diamagnetic behavior, the superconducting volume fraction is lower than 1% (inset). The full superconducting volume fraction is reached with a $\approx 0.5\%$ increase of x , i.e. at $x \approx 0.0366$, attesting once more to the high quality of the crystals. The value of doping for which superconductivity is stabilized is in good agreement with values from the literature²⁷.

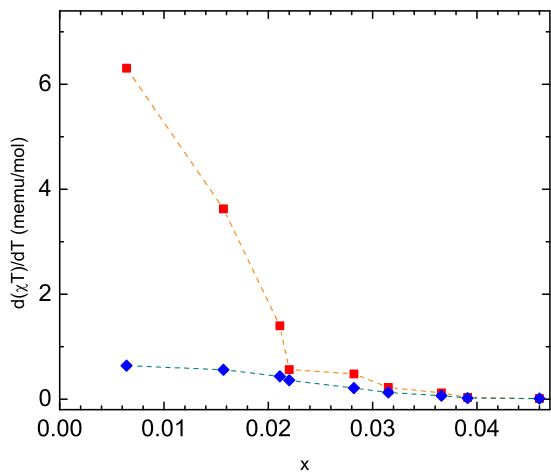


FIG. 4: The $d(\chi T)/dT$ magnitudes at T_N (■) and T_s (◆) of $\text{BaFe}_2(1-x)\text{Co}_{2x}\text{As}_2$ versus x , for $0.0064 \leq x \leq 0.046$.

Figure 4 shows the magnitudes of $d(\chi T)/dT$ at $T=T_N$ (■) and at $T=T_s$ (◆) of $\text{BaFe}_2(1-x)\text{Co}_{2x}\text{As}_2$ versus x for $0.0064 \leq x \leq 0.0391$. The $x=0$ point is not included in the

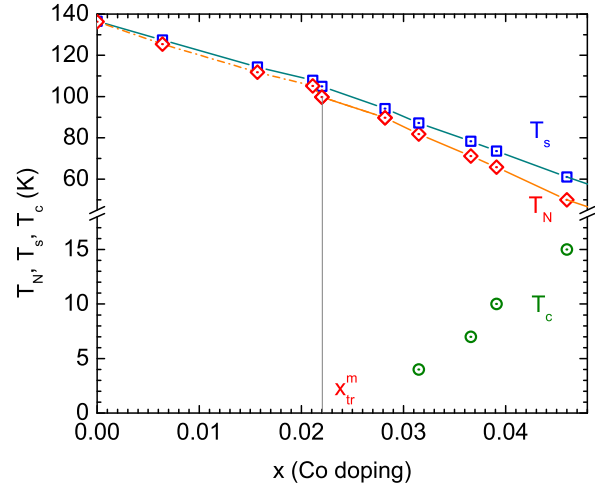


FIG. 5: The phase diagram for the doping range near the tricritical points. For T_s and T_N the discontinuous line indicates first order transition and the continuous line second order transition.

graph since the peak associated with the onset second order structural transition could not be separated from the large first order jump. For $d(\chi T)/dT(T=T_N)$ the crossover points x_{tr} marks the separation between a globally abrupt and non-monotonic doping evolution (characteristic of 1st order transitions region) and a monotonic variation (region characteristic of 2nd order transitions). The magnetic crossover at $x_{tr}^m \approx 0.022$, appears to be a tricritical point; this confirms, albeit with much more precision, the suggestion of Kim *et al.*¹⁴. Any possible structural crossover is more difficult to discuss given that at $x=0$ the transition is characterized by a second order onset followed by a large first order jump presumably driven by the first order magnetic transition. At $x^s \approx 0.0064$ the heat capacity of the second order structural transition becomes clearly visible. Figure 5 summarize the above results in a phase diagram (T x). For T_s and T_N the discontinuous line indicates first order transition and the continuous line second order transition. The phase diagram here is similar to the one for the 122s predicted by Cano *et al.*²⁸. Their Ginzburg-Landau model contains a magnetoelastic coupling term as a key ingredient. Using a slight variation of the afore mentioned model, Kim *et al.*¹⁴ predicted that the magnetic tricritical point is $x \approx 0.022$. It should be noted that Wilson *et al.*⁴ have shown that in BaFe_2As_2 below the first order transition the magnetic and structural order parameters exhibit identical temperature dependencies. This requires that there is a dominant biquadratic coupling between the magnetic and structural order parameters. The biquadratic term is not included in the above-mentioned theories.

In summary we have systematically studied the magnetic susceptibility of high quality $\text{BaFe}_{2(1-x)}\text{Co}_{2x}\text{As}_2$, $0 \leq x \leq 0.046$ as grown single crystals. Our measurements confirm the existence of a magnetic tricritical point at the cobalt doping $x \approx 0.022$. They also demonstrate that the anomaly associated with the putative second order structural transition emerges clearly separated from the first order combined magnetic and structural transition at a doping of about 0.0064. We show further that the superconductivity emerges at higher cobalt doping than

that at the magnetic tricritical point: namely $x \approx 0.0315$.

We thank Dung-Hai Lee, Alan I. Goldman, and Jörg Schmalian for valuable communications about their results and to Edith Bourret and John Heron for assistance. This work was supported by the Director, Office of Science, Office of Basic Energy Sciences, U.S. Department of Energy, under Contract No. DE-AC02-05CH11231 and Office of Basic Energy Sciences US DOE DE-AC03-76SF008.

-
- * E-mail address: CRRotundu@lbl.gov
- ¹ A. S. Sefat, R. Jin, M. A. McGuire, B. C. Sales, D. J. Singh, and D. Mandrus, *Phys. Rev. Lett.* **101**, 117004 (2008).
 - ² J.-H. Chu, J. G. Analytis, C. Kucharczyk, and I. R. Fisher, *Phys. Rev. B* **79**, 014506 (2009).
 - ³ M. Rotter, M. Tegel, D. Johrendt, I. Schellenberg, W. Hermes, and R. Pöttgen, *Phys. Rev. B* **78**, 020503(R) (2008).
 - ⁴ S. D. Wilson, Z. Yamani, C. R. Rotundu, B. Freelon, E. Courchesne, and R. J. Birgeneau, *Phys. Rev. B* **79**, 184519 (2009).
 - ⁵ K. Kitagawa, N. Katayama, K. Ohgushi, M. Yoshida, and M. Takigawa, *J. Phys. Soc. Jpn.* **77**, 114709 (2008).
 - ⁶ K. Matan, R. Morinaga, K. Iida, and T. J. Sato, *Phys. Rev. B* **79**, 054526 (2009).
 - ⁷ C. R. Rotundu, B. Freelon, T. R. Forrest, S. D. Wilson, P. N. Valdivia, G. Pinuellas, A. Kim, Z. Islam, J. -W. Kim, E. Courchesne, N. E. Phillips, and R. J. Birgeneau, *Phys. Rev. B* **82**, 144525 (2010).
 - ⁸ D. K. Pratt, W. Tian, A. Kreyssig, J. L. Zarestky, S. Nandi, N. Ni, S. L. Bud'ko, P. C. Canfield, A. I. Goldman, and R. J. McQueeney, *Phys. Rev. Lett.* **103**, 087001 (2009).
 - ⁹ S. Nandi, M. G. Kim, A. Kreyssig, R. M. Fernandes, D. K. Pratt, A. Thaler, N. Ni, S. L. Bud'ko, P. C. Canfield, J. Schmalian, R. J. McQueeney, and A. I. Goldman, *Phys. Rev. Lett.* **104**, 057006 (2010).
 - ¹⁰ L. W. Harriger, A. Schneidewind, S. Li, J. Zhao, Z. Li, W. Lu, X. Dong, F. Zhou, Z. Zhao, J. Hu, and P. Dai, *Phys. Rev. Lett.* **103**, 087005 (2009).
 - ¹¹ G. Giovannetti, C. Ortix, M. Marsman, M. Capone, J. van den Brink, and J. Lorenzana, arXiv:1009.0009v1 (unpublished).
 - ¹² S. Avci, O. Chmaissem, E. A. Goremychkin, S. Rosenkranz, J.-P. Castellán, D. Y. Chung, I. S. Todorov, J. A. Schlueter, H. Claus, M. G. Kanatzidis, A. Daoud-Aladine, D. Khalyavin, and R. Osborn, arXiv:1102.1933 (unpublished).
 - ¹³ C. Liu, T. Kondo, R. M. Fernandes, A. D. Palczewski, E. D. Mun, N. Ni, A. N. Thaler, A. Bostwick, E. Rotenberg, J. Schmalian, S. L. Bud'ko, P. C. Canfield and A. Kaminski, *Nature Physics* **6**, 419 (2010).
 - ¹⁴ M. G. Kim, R. M. Fernandes, A. Kreyssig, J. W. Kim, A. Thaler, S. L. Bud'ko, P. C. Canfield, R. J. McQueeney, J. Schmalian, and A. I. Goldman, *Phys. Rev. B* **83**, 134522 (2011).
 - ¹⁵ M. T. Dove, *Structure and Dynamics – An atomic view of materials*, Oxford University Press, Cambridge, UK (2010).
 - ¹⁶ Critical exponents are not defined at a first-order transition.
 - ¹⁷ A. Kozłowski, Z. Kąkol, R. Zalecki, K.S. Knight, and J.M. Honig, *J. Phys. IV France* **7**, 591 (1997).
 - ¹⁸ A. Kozłowski, Z. Kąkol, R. Zalecki, K. S. Knight, J. Sabol and J. M. Honig, *J. Phys.: Condens. Matter* **11**, 2749 (1999).
 - ¹⁹ M. C. Gallardo, F. J. Romeo, S. A. Hayward, E. K. Salje, and J. del Cerro, *Mineralogical Magazine* **64**, 971 (2000).
 - ²⁰ The latent heat is the thermodynamic measure that determines the first-order character of a phase transition.
 - ²¹ J. del Cerro, F.J. Romero, M.C. Gallardo, S.A. Hayward, J. Jiménez, *Thermochim. Acta* **343**, 89 (2000).
 - ²² F. J. Romero, M. C. Gallardo, J. Jiménez, J. del Cerro, *Thermochim. Acta* **372**, 25 (2001).
 - ²³ M. E. Fisher, *Philosophical Magazine* **7**, 1731 (1962).
 - ²⁴ X. F. Wang, T. Wu, G. Wu, H. Chen, Y. L. Xie, J. J. Ying, Y. J. Yan, R. H. Liu, and X. H. Chen, *Phys. Rev. Lett.* **102**, 117005 (2009).
 - ²⁵ MPMS Application Note 1014-210B, 03-04-1997.
 - ²⁶ S. Gregory, *Phys. Rev. Lett.* **40**, 723 (1978).
 - ²⁷ N. Ni, M. E. Tillman, J.-Q. Yan, A. Kracher, S. T. Hannahs, S. L. Bud'ko, and P. C. Canfield, *Phys. Rev. B* **78**, 214515 (2008).
 - ²⁸ A. Cano, M. Civelli, I. Eremin, and I. Paul, *Phys. Rev. B* **82**, 020408(R) (2010).